Determination of Size Distributions of Concentrated Polymer Particles Embedded in a Solid Polymer Matrix

Ezequiel R. Soulé, Guillermo E. Eliçabe*

(Received: 3 July 2007; in revised form: 18 September 2007; accepted: 18 September 2007; published online: 7 February 2008)

DOI: 10.1002/ppsc.200700003

Abstract

In this work we present the results obtained from the size characterization of polymer particles embedded in a solid polymer matrix using Static Light Scattering (SLS) and Scanning Electron Microscopy (SEM). The analyzed samples are the result of the solution polymerization of isobornyl methacrylate (IBoMA) in polyisobutylene (PIB) at complete conversion. Induced by polymerization, the system undergoes phase separation. As a result, spherical micron sized particles rich in PIB are formed. At the end of the polymerization, the particles become trapped in a solid polymer matrix rich in Poly-IBoMA. Size, concentration, and refractive index, make the resulting particle system scatter light under the Rayleigh-Debye-Gans (RDG) regime with interparticle interference. For Light Scattering (LS) characterization the samples are measured with a Flat Cell Static Light Scattering (FCSLS) apparatus, in which the reaction takes place. The resulting SLS spectra are analyzed using the Percus-Yevick approximation to model the interference effects. The local monodisperse approximation is used to consider polydispersity in the particle sizes. The estimated particle size distributions agree well with the measurements from SEM. In this work a concentrated particle system that naturally scatters light according to the RDG regime has been fully characterized in terms of its particle size distribution. This work, against the opinion of other authors, shows the feasibility of measuring still particles using a one dimensional array of light detectors.

Keywords: concentrated particles, polymer phase separation, size distributions, static light scattering

1 Introduction

Scattering methods have been used extensively to investigate colloidal systems and complex fluids [1]. In particular, Static Light Scattering (SLS) has proved to be an excellent choice when sizing particles in a range from 100 nm to 10 μm. If the concentration of particles is low, single and independent scattering are valid and Mie theory can be used to precisely describe the scattering phenomenon [2–4]. When the concentration of particles is high and cannot be modified by dilution, the assumptions of single and independent scattering are, in general, not valid. However, if the particles are small compared to the wavelength of the incident light or the optical contrast between the particles and the surrounding medium is small, multiple scattering can be neglected up to relatively high concentrations and only particle interference needs to be considered [5]. The scattering of light in these cases can be correctly described by the Rayleigh-Debye-Gans (RDG) theory [6]. The RDG theory is particularly applicable to scattering of X-rays and neutrons, because in these techniques the restrictions imposed for the scattering of light are practically removed. For this reason, there are many applications of the RDG theory in the field of particle sizing using scattering data from X-rays or neutrons. The results from these applications can be directly extended to the analysis of light scattering data as far as the restrictions imposed on this type of data are fulfilled.

* Prof. G. E. Elicabe (corresponding author), Dr. E. R. Soulé, Institute of Materials Science and Technology (INTEMA), University of Mar del Plata and National Research Council (CONICET), J. B. Justo 4302, 7600 Mar del Plata (Argentina).
E-mail: elicabe@fi.mdp.edu.ar

The rigorous application of RDG theory to systems with interactions and polydispersity in the particle sizes is complex and the resulting equations are quite involved [7]. For that reason, different approximations have been proposed. In the 'decoupling approximation' [8], it is assumed that the positions of the particles are independent of their sizes. This approach gives reasonable results for small polydispersities. The 'monodisperse approximation' [9] is built on the assumption that the positions of the particles are completely correlated with their sizes, i.e., the system is approximated by many subsystems in which the particles are monodisperse. This approach gives a more realistic smearing of the interference effects due to the inclusion of polydispersity and therefore works better for larger polydispersities. This approach was applied to the evaluation of neutron scattering data with good results [9]. In a more recent publication, the pair distance distribution functions of several interacting spherical and non-spherical particle systems are obtained from numerically generated data of neutron scattering experiments [10]. A polidispersity parameter is included in the structure factor together with the volume fraction, the radius, and the charge of the particles. In particular, good results are obtained for the estimation of the particle volume distribution of homogeneous spheres. The numerical approach presented in this article also has been used for the determination of the pair distance distribution function of concentrated micrometer-sized oil-in-water emulsions using light scattering [5]. In this article, in order to analyze the particle system using RDG theory, the samples must be nearly index-matched by the addition of appropriate substances. This option, which in some cases is less disturbing than dilution, may not be applicable in other systems. For this reason, the analysis of concentrated particle systems using light scattering is limited by these constraints.

However, some concentrated particle systems, like those that arise in a phase separation in a polymer system, in which the optical contrast between particles and surrounding medium is naturally low, are excellent candidates to be evaluated using the theory and methods described above. This is because the refractive indices of the polymers involved are in many cases very similar. In fact, there are several applications of SLS that allow one to follow the morphological evolution of a variety of phase separating polymer systems that produce concentrated particle systems [11]. In many cases the Light Scattering (LS) spectra obtained during phase separation are simply correlated with the qualitative knowledge available on these systems to infer their morphologies [12]. In a few others, some quantitative results are obtained using mathematical models of the scattering phenomena [13]. Particle size characterization in phase separating polymer systems has recently been used to understand different characteristics of the analyzed system: from kinetic mechanisms to morphological conformation [14]. However, as far as the authors know, there is no comprehensive study in which particle size distributions in phase separated polymer systems are estimated using detailed models of the light scattering process.

In this work we present the results obtained from the size characterization of polymer particles embedded in a solid polymer matrix using SLS and Scanning Electron Microscopy (SEM). For LS characterization the samples are measured with a Flat Cell Scanning Light Scattering (FCSLS) apparatus built in our laboratory [15]. The analyzed samples are the result of the solution polymerization of isobornyl methacrylate (IBoMA) in polyisobutylene (PIB) at complete conversion. The polymerization is carried out in the FCSLS apparatus. As the system reacts, phase separation, induced by polymerization, occurs. As a result, spherical micron sized particles rich in PIB are formed. At the end of the polymerization process, when vitrification occurs, the particles become trapped in a solid polymer matrix rich in Poly-IBoMA. The resulting solid sample can also be precisely characterized using SEM.

The use of the RDG theory to model the experimental results obtained with the particle system studied here is supported by the results reported in reference [5]. In that work a transition from RDG regime to Mie theory is verified for samples with particle radii, R, of about 0.5 μm. The study indicates that when the relative refractive index of the particles, m, is equal to 1.04 the particle size distributions estimated with the RDG and Mie theories are very similar. As m increases, the estimations using RDG theory tend to shift to larger sizes indicating that this theory is no longer valid. Because in our case m is no larger than 1.02 and the mean radii, $\bar{R}$, is in all cases smaller than in that study, we assume that RDG is a valid approach to investigate the particle system proposed here.

In this work the effect of particle concentration on scattered light must also be considered through the evaluation of interparticle interference [6, 16]. Thus, the resulting SLS spectra are analyzed using the Percus-Yevick approximation [17] to model the interference effects. The local monodisperse approximation [9] is used to consider polydispersity in the particle sizes.

2 Theory

2.1 Light Scattering

Independent single scattering by a system of spherical particles can be precisely described by the so-called Mie theory [2–4]. However, when the concentration of particles is high and cannot be controlled by dilution, the assumptions of single and independent scattering may be no longer valid.

If the particles are small compared to the wavelength of the incident light, multiple scattering can be neglected up to relatively high concentrations and particle interactions can be taken into account by the RDG theory. Scattering by micrometer-sized systems cannot be analyzed using the RDG equations unless the refractive index of the particles is very close to that of the suspending medium. If this occurs, again multiple scattering becomes important only at higher concentrations than particle interactions do, and then scattering at moderate concentrations can also be treated using the RDG theory [5]. In general this theory can be used when $2a(m-1) << 1$. Where a, the size parameter, is defined as $\frac{2\pi R n_m}{\lambda_0}$; λ_0 is the wavelength of the incident light in vacuum; and $m = \frac{n_p}{n_m}$ is the refractive index ratio of the particles, n_p, relative to the refractive index of the suspending medium n_m.

The light scattered under the RDG regime after correction for the polarization of the incident light [4], for a collection of N spherical particles can be expressed as

$$I_s(\theta,\phi) \sim \left| \sum_{i=1}^{N} F_i(q) e^{-j\mathbf{q}\cdot\mathbf{r}_i} \right|^2 \tag{1}$$

where $F_i(q)$, the form factor of the i sphere of radius R_i, is given by

$$F_i(q) = \frac{1}{q} \int_0^{R_i} r \sin qr \, dr = \frac{1}{q^3} (\sin qR_i - qR_i \cos qR_i) \tag{2}$$

In the above equations $\mathbf{q} = \mathbf{q}_f - \mathbf{q}_0$, where $\mathbf{q}_f$ and $\mathbf{q}_0$ are vectors of magnitude $2\pi n_m/\lambda_0$, pointing the former from the center of each particle to the detector, and the latter in the direction of the incident light. q is the magnitude of $\mathbf{q}$ ($|\mathbf{q}| = \frac{4\pi n_m}{\lambda_0} \sin \frac{\theta}{2}$), θ the scattering angle, ϕ the azimuthal angle, and $\mathbf{r}_i$ is the position vector of the center of particle i.

If the particles are all of the same size, $R_i = R$ for $i = 1 \ldots N$, then the scattered light is given by

$$I_s(\theta,\phi) \sim [F(q)]^2 \, S(q) \tag{3}$$

where the structure factor, $S(q)$, is given by

$$S(q) \sim \left| \sum_{i=1}^{N} e^{-j\mathbf{q}\cdot\mathbf{r}_i} \right|^2 \tag{4}$$

The structure factor can be computed using the closed-form solution of the Percus-Yevick equation [17]:

$$S(q) = \frac{1}{1 - N_p (2\pi)^3 C(q)} \tag{5}$$

where

$$N_p(2\pi)^3 C(q) = 24p \left\{ \frac{(\alpha+\beta+\delta)}{u^2} \cos u - \frac{(\alpha+2\beta+4\delta)}{u^3} \sin u - \frac{2(\beta+6\delta)}{u^4} \cos u + \frac{2\beta}{u^4} + \frac{24\delta}{u^5} \sin u + \frac{24\delta}{u^6} (\cos u - 1) \right\} \tag{6}$$

and

$$u = 2qR \tag{7}$$

$$\alpha = \frac{(1+2p)^2}{(1-p)^4} \tag{8}$$

$$\beta = -6p \frac{(1+\frac{p}{2})^2}{(1-p)^4} \tag{9}$$

$$\delta = \frac{p(1+2p)^2}{2(1-p)^4} \tag{10}$$

N_p is the number of particles per unit volume and $p = N_p 4/3\pi R^3$ is the volume fraction of particles in the system.

When the particle system is polydisperse one should deal with partial structure factors [18]. However, the use of these factors makes the computational problem too complex to be included in a scheme to be used in least squares analysis. For this reason, several approximations have been proposed in order to avoid the use of partial structure factors. In this work the so-called monodisperse approximation [9], which considers that the scattering intensity is given as the incoherent sum of the scattering intensities of the monodisperse subsystems weighted with the size distribution, is used. Thus, given a number particle size distribution $f(R)$,

$$I_s(q) \sim \int_0^{\infty} f(R) S(q,R,p) \, F^2(q,R) dR \tag{11}$$

In this equation p must be considered as an apparent parameter which value is closer to the actual volume fraction as the polydispersity of the particle sizes is small. In reference [9] this approximation has been tested in the context of the evaluation of hard-sphere models, with relatively good results.

2.2 Parameter Estimation

In order to compute the parameters of interest from the LS spectra, Eq. (11) must include a prefactor that depends on some of the model parameters. It can be shown that this prefactor is given by

$$K = K_C \, \Delta n^2 N_p \tag{12}$$

Where Δn is the difference in refractive index between the particles and the suspending medium, K_C is an instrument dependent parameter, usually unknown, and N_p is the number of particles per unit volume. If Eq. (12) is to hold, it is implicit that $f(R)$ is normalized to have an area equal to one.

Thus the parameters to be estimated are: K, p, R_0, and g. The last two define the shape of the log-normal distribution used in this study:

$$f(R) = \frac{(g/\pi)^{1/2}}{R} \exp\left\{ -g[\log(R/R_0)]^2 \right\} \quad (13)$$

Note that the distribution in this form is not normalized. Mean and variance are given by $\bar{R} = R_0 \exp(\frac{1}{4g})$ and $\sigma^2 = 2R_0^2 \exp(\frac{3}{4g}) \sinh(\frac{1}{4g})$.

3 Experimental

3.1 Materials

Isobornyl methacrylate (IBoMA, Aldrich) was used as received. It contained 150 ppm of *p*-methoxyphenol (MEHQ, methyl ether hydroquinone) as inhibitor. Its mass density at 15 °C was ρ_{IBoMA} = 0.983 g/cm^3 and its refractive index was n_{IBoMA} = 1.48. Benzol peroxide (BPO, Akzo-Nobel) was used as initiator. Two commercial poly(isobutylenes) (PIB, Repsol YPF, Argentina) labeled PIB5 and PIB025, were used. Molar mass distributions were reported by the supplier. Their molar mass averages were: M_n = 808, M_w = 1912, and M_z = 5164 for PIB5, and M_n = 674, M_w = 1033, and M_z = 1490 for PIB025. Their mass densities at 15 °C were 0.888 g/cm^3 for PIB5 and 0.875 for PIB025, and their refractive indices were 1.51 for PIB5 and PIB025.

3.2 Scanning Electron Microscopy and SEM

The FCLS apparatus consists of a linear array of photodiodes placed to detect the light scattered by a thin sample illuminated by a 17 mW He-Ne laser with random polarization. The laser beam is attenuated by a neutral density filter, expanded by a 5x beam expander and trimmed by an iris diaphragm before reaching the sample. The sample holder is made of two glass windows separated by a 1.2 mm spacer and placed in an aluminum block provided with a computer-controlled electrical heating system. The light scattered from the sample is collected by 14 cathode monolithic silicon photodiode linear arrays of 16 elements each, manufactured by Photonics Detectors Inc. The arrays, of length 25.20 mm each, are located one next to the other with a small gap of 0.25 mm. The active area of each element is 2.31 mm^2. Every photodiode operates as a current source linearly controlled by the light intensity. An opal diffusing glass is used to calibrate the photodiodes individually and thus compensate for their different gains. The current from the photodiode circulates through a resistance generating a voltage proportional to the incident light. This voltage is sensed by 29 integrated circuits, consisting of an 8-channel multiplexer and a 12-Bit A/D converter. Serial communication is used to receive the control signals employed to select the channel that is sampled. Signals are sent to a microprocessor that carries out all the coordination and control tasks, connected to a personal computer through a serial port. This type of connection imposes a minimum sampling time of 1 s, although the time needed to collect a whole spectrum is much less.

Blends with: a) 30 wt% PIB5 in IBoMA (30PIB5), b) 50 wt% PIB5 in IBoMA (50PIB5), and c) 50 wt% PIB025 in IBoMA (50PIB025), were used in the rest of this study. Each formulation was placed in the sample holder and temperature was raised to 80 °C and kept constant. As polymerization takes place, LS spectra were recorded. After several hours, all perceptible signs of change in scattered light disappear. At that point, the sample has vitrified and can be cooled down up to ambient temperature without observing noticeable changes in the light spectrum. An average of the spectra recorded after vitrification is used for sample characterization.

For EM, the resulting solid samples were extracted from the sample holder and fractured. SEM micrographs of fracture surfaces coated with a fine gold layer were obtained using a Jeol JSM 6460 LV device.

4 Results and Discussion

Eq. (11), including the prefactor described in Eq. (12) and corrected with a term proportional to q^{-2}, was used to fit the measured spectra. This term accounts for the spectra without particles and includes optical effects such as the grazing incidence of the light and the finite size of the diode elements and scattering by impurities. The square law for the background is supported by the fact that this form gives the best fit to the blank spectra taken when each sample is measured before any particle is present, at the beginning of the polymerization. In this form, five parameters are estimated for each spectrum: K, p, R_0, g and a, where a is the prefactor of q^{-2}. In all the analyzed cases the fit to the data starts at q = 1.77 μm^{-1}, in order to avoid the intensities too close to the incident direction, because they are the more distorted ones.

In Figure 1a) the LS spectrum corresponding to formulation 30PIB5 is shown together with the model fit. A decomposition of the curve that fits the data in a part that corresponds to the particles (Eq. 11) and a part to the spectra without particles is also shown. As can be seen, the fit to the data is excellent. In Figure 1b) the normalized particle size distribution estimated from the LS spectrum is shown together with the one determined

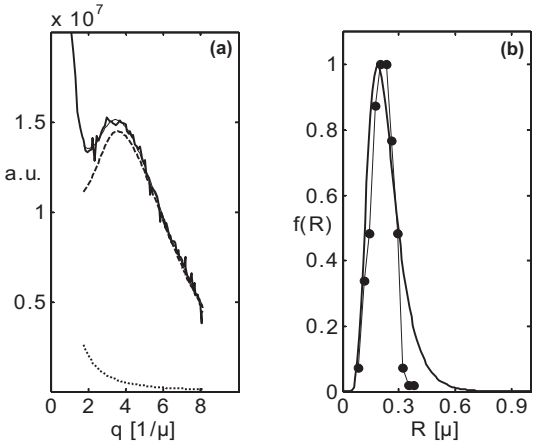

Fig. 1: Results for formulation 30PIB5: (a) Experimental LS data (thick full curve); fit of the model (thin full curve); fit of the model corresponding to the particles (dashed curve); and fit of the model corresponding to the spectrum without particles (dotted curve). (b) Normalized particle size distribution estimated from model fitting (thick full curve); normalized particle size distribution calculated from SEM (thin full curve with full circles).

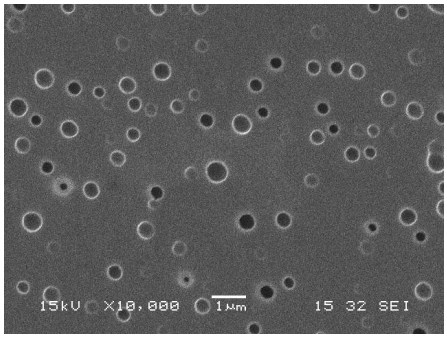

Fig. 2: SEM micrograph of sample 30PIB5.

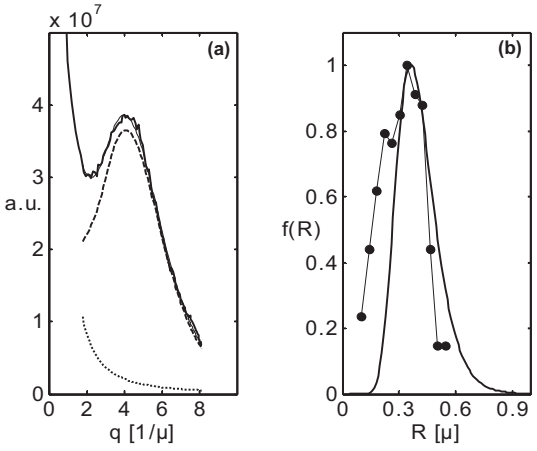

Fig. 3: Results for formulation 50PIB5: (a) Experimental LS data (thick full curve); fit of the model (thin full curve); fit of the model corresponding to the particles (dashed curve); and fit of the model corresponding to the spectrum without particles (dotted curve). (b) Normalized particle size distribution estimated from model fitting (thick full curve); normalized particle size distribution calculated from SEM (thin full curve with full circles).

using SEM. The estimated distribution from LS is in agreement with that determined by SEM in almost the whole range of sizes. Some discrepancy is noted at the larger particle radii: a tail of large particles not observed under SEM is estimated by LS. A possible explanation of this disagreement may be attributed to the rigidity imposed by the fix-form determination proposed here for the particle size distribution. Another possible source of error may be related to the approximated nature of the model with regard to the form in which the polydispersity of the particle sizes is taken into account. In Figure 2 a SEM micrograph of the sample is also shown. In this micrograph a rather concentrated system of spherical polydisperse particles can be clearly noticed.

Figures 3a) and 3b) show the results corresponding to formulation 50PIB5. As before, the model fitting is excellent. In this case, the estimated particle size distribution deviates somewhat at the smaller particle radius from the distribution determined by SEM. However, the position of the maximum is correctly predicted by the model. Part of the deviation may be attributed to the same reasons as those given for sample 30PIB5. However, in this example a more specific source of error that originates in the discrepancies between the real morphologies of the particles with respect to the homogenous sphere assumed in the LS model may contribute to a greater extent to the deviations mentioned before. In Figure 4 a SEM micrograph of the sample is also shown. A more concentrated system of larger particles than that of sample 30PIB5 can be observed in this micrograph. It can also be observed in a few of the particles that small holes are present on the surface. This is evidence of secondary phase separation that could have taken place during the conformation of the solid sample analyzed here, giving rise to a system of spherical particles with spherical inclusions, and thus violating the assumptions of the model.

The LS spectra, the fits of the model and the normalized particle size distributions for two samples of blend

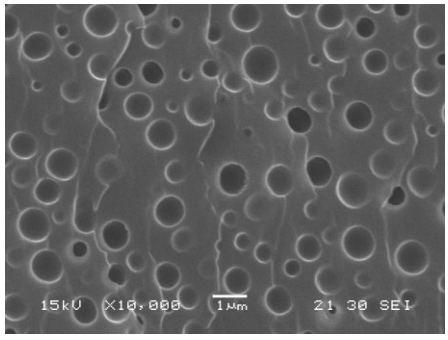

Fig. 4: SEM micrograph of sample 50PIB5.

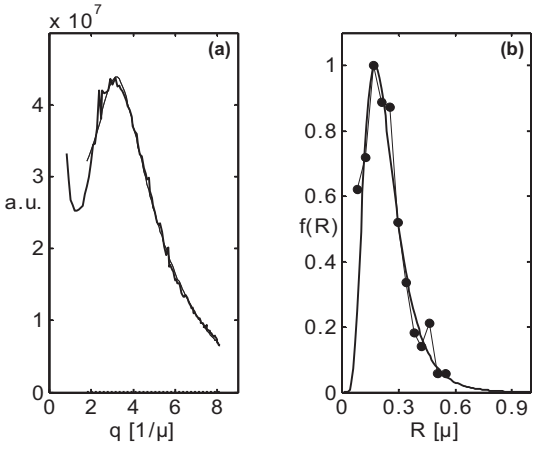

Fig. 5: Results for formulation 50PIB025: (a) Experimental LS data (thick full curve); fit of the model (thin full curve). (b) Normalized particle size distribution estimated from the model fitting (thick full curve); normalized particle size distribution calculated from SEM (thin full curve with full circles).

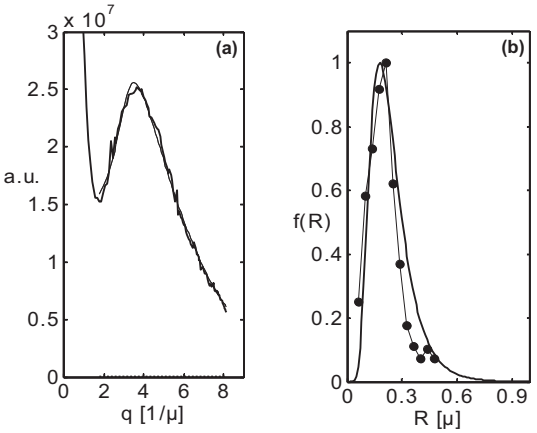

Fig. 7: Results for formulation 50PIB025 (replica): (a) Experimental LS data (thick full curve); fit of the model (thin full curve). (b) Normalized particle size distribution estimated from the model fitting (thick full curve); normalized particle size distribution calculated from SEM (thin full curve with full circles).

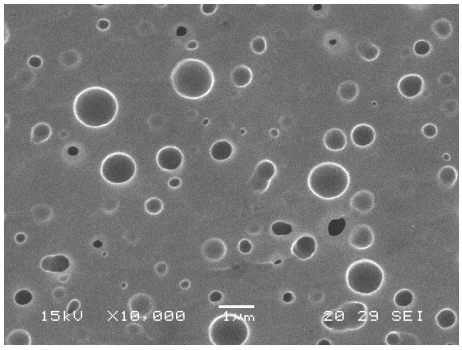

Fig. 6: SEM micrograph of sample 50PIB025.

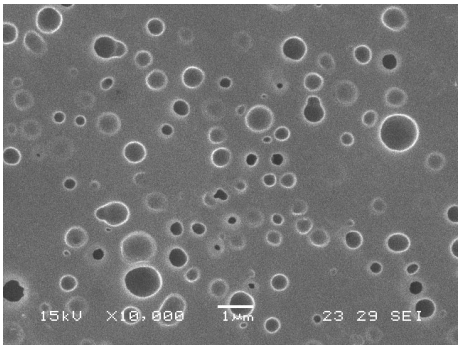

Fig. 8: SEM micrograph of sample 50PIB025 (replica).

50PIB025 are shown in Figures 5 and 7. The fit to the data is excellent and the estimated distributions agree very well with those determined with SEM. The estimated spectra without particles are in these two cases negligible. Figures 6 and 8 show SEM micrographs of these samples. Although the mean values of the particle size distributions are very similar to that of sample 30PIB5, larger and smaller particles than in that sample can be easily distinguished in the micrographs, implying a larger polydispersity.

In Table 1, the estimated values of $\bar{R}$, σ, p, K and a for the four blends tested here are shown. The values of $\bar{R}$, σ and p calculated from the SEM micrographs are also reported. The studied samples present three different characteristics, small particles and standard deviation (30PIB5), large particles and standard deviation (50PIB5), and small particles and large standard deviation (50PIB025). Except for the mean radius of sample 50PIB5 and the standard deviation of sample 30PIB5, the small difference between the estimated and calculated parameters of the particle size distributions reflects the good agreement between the corresponding distributions. These results, however, are not conclusive evidence of the capability of SLS to assess a range of polydispersities because they are very similar in all the

Table 1: Estimated parameters from SLS and measured parameters from SEM, for the four samples analyzed.

	30PIB5		50PIB5		50PIB025		50PIB025 (replica)	
	SLS	SEM	SLS	SEM	SLS	SEM	SLS	SEM
$\hat{K}$	1e12	–	2.9e11	–	1.6e12	–	1.5e12	–
$\hat{p}$	0.28	0.052	0.35	0.15	0.29	0.085	0.35	0.077
$\hat{\bar{R}}$ [μ]	0.24	0.21	0.40	0.31	0.24	0.23	0.24	0.19
$\hat{\sigma}$ [μ]	0.096	0.054	0.11	0.11	0.12	0.12	0.11	0.091
$\hat{a}$	8.1e06	–	3.4e07	–	0.12	–	1.3e-06	–

samples. As expected, the estimated volume fraction of particles in the system, p, is very different from the one calculated by SEM. In the model, p, more than a physical parameter, must be considered as an effective parameter describing the interference effects in the presence of polydispersity. Parameter K was estimated without normalizing $f(R)$. This parameter and a can not easily be checked independently and their values are reported just for completeness.

5 Conclusions

As a non-invasive technique, SLS may be very convenient for estimating particle size distributions in phase separating polymer systems when the study must be performed while particles and medium remain liquid. In order to validate the models used for estimation it is desirable to use other characterization methods. SEM is a good alternative technique only if one of the phases is solid. In most cases, when phase separation is induced by polymerization, at the end of the reaction at least one of the phases becomes solid.

In this work we have validated a light scattering model based on the Percus-Yevick and "local monodisperse" approximations for the particle system that originates at the end of the polymerization of isobornyl methacrylate in the presence of polyisobutylene. RDG theory was legitimately applied because of the naturally low optical contrast present in heterogeneous polymer systems. Validation using SEM was possible because the resulting particle system consists of particles rich in PIB embedded in a solid polymer matrix rich in Poly-IBoMA. This validation can be in part extended to previous stages of the polymerization when both phases are liquid, because the characterized solid system still preserves many of the characteristics of the liquid one; i.e. particle size, particle concentration, and to some extent, particle-matrix optical contrast.

It has been reported in the literature [19] that systems of immobile particles like the ones analyzed here may display an important level of speckle effect when scattered light is measured with linear arrays of diodes. Speckle effect may negatively impact on the quality of the measured LS spectra. However, in this work we have demonstrated that a proper combination of sample size and incident beam expansion helps to minimize speckle and makes our FCSLS appropriate to characterize the solid particle systems studied here.

6 Nomenclature

a	prefactor of q^{-2}
f	number particle radii distribution
F	form factor
g	parameter of lognormal distribution
I_s	scattered light
K	prefactor
K_C	instrument dependent parameter
m	relative refractive index
M_n	number average molar mass
M_w	weight average molar mass
M_z	z-average molar mass
n_m	refractive index of the suspending medium
n_p	refractive index of the particles
N	number of particles
N_p	number of particles per unit volume
p	volume fraction of particles
q	magnitude of scattering vector
$\mathbf{q}$	scattering vector
r	integration variable
$\mathbf{r}$	position vector of the center of a particle
R	particle radius
$\bar{R}$	mean of particle radii distribution
R_0	parameter of lognormal distribution
S	structure factor
^	estimated values
α	size parameter
Δn	difference in refractive index between the particles and the suspending medium
θ	scattering angle
λ_0	wavelength of the incident light in vacuum
ρ	mass density
σ^2	variance of particle radii distribution
ϕ	azimuthal angle
BPO	Benzol PerOxide
FCSLS	Flat Cell Static Light Scattering
IBoMA	IsoBornyl MethAcrylate
LS	Light Scattering
MEHQ	Methyl Ether HydroQuinone
PIB	Poly(IsoButylene)
RDG	Rayleigh-Debye-Gans
SEM	Scanning Electron Microscopy
SLS	Static Light Scattering

7 Acknowledgment

We acknowledge the financial support of the following institutions in Argentina: University of Mar del Plata, National Research Council (CONICET), and National Agency for the Promotion of Science and Technology (ANPCyT).

8 References

[1] P. Lindner, T. Zemb, *Neutrons, X-rays and Light scattering Methods Applied to Soft Condensed Matter*. Elsevier Science, Amsterdam, **2002**.

[2] H. C. van de Hulst, *Light scattering by Small Particles*. Dover Publications, New York, **1981**.

[3] M. Kerker, *The Scattering of Light and Other Electromagnetic Radiation*. Academic Press, New York, **1969**.

[4] C. Bohren, D. Huffman, *Absorption and Scattering of Light by Small Particles*. John Wiley & Sons, **1983**.

[5] H. Lindner, G. Fritz, O. Glatter, Measurements on Concentrated Oil in Water Emulsions Using Scanning Electron Microscopy. *J. Colloid Interf. Sci.* **2001**, *242*, 239–246.

[6] E. K. Hobbie, L. Sung, Rayleigh-Gans Scattering from Polydisperse Colloidal Suspensions. *Am. J. Phys.* **1996**, *64*, 1298–1303.

[7] J. S. Pedersen, Small-Angle Scattering from Precipitates: Analysis by Use of a Polydisperse Hard-Sphere Model. *Phys. Rev. B* **1993**, *47*, 657–665.

[8] M. Kotlarchyck, Sow-Hsin Chen, Analysis of Small Angle Neutron Scattering Spectra from Polydisperse Interacting Colloids. *J. Chem. Phys.* **1983**, *79*, 2461–2469.

[9] J. S. Pedersen, Determination of Size Distribution from Small-Angle Scattering Data for Systems with Effective Hard-Sphere Interactions. *J. Appl. Cryst.* **1994**, *27*, 595.

[10] J. Brunner-Popela, O. Glatter, Small-Angle Scattering of Interacting Particles. I. Basic Principles of a Global Evaluation Technique. *J. Appl. Cryst.* **1997**, *30*, 431–442.

[11] T. Kyu, Time-Resolved Characterization of Polymer Phase Transitions, in *Comprehensive Polymer Science, 2nd Supplement* (Eds.: S. L. Aggarwal and S. Russo), Elsevier Science, **1996**, 307–345.

[12] L. Baeke, P. Thioudelet, P. Keates, P. Navard, A Depolarized Light Scattering Study of the Phase Separation Process in an Epoxi-Elastomer Blend. *Polymer* **1997**, *38*, 5283–5287.

[13] R. H. Tromp, R. A. L. Jones, Off-Critical Phase Separation and Gelation in Solutions of Gelatin and Dextran. *Macromolecules* **1996**, *29*, 8109–8116.

[14] E. R. Soulé, G. E. Eliçabe, J. Borrajo, R. J. J. Williams, Analysis of the Phase Separation Induced by a Free-Radical Polymerization in Solutions of Polyisobutylene in Isobornyl Methacrylate. *I&EC*, **2007** (in press).

[15] G. E. Eliçabe, W. F. Schroeder, G. L. Frontini, V. Pettarin, Particle Systems Characterization Using a Flat Cell Scanning Electron Microscopy Apparatus. *Part. Part. Syst. Charact.* **2007** (in press).

[16] G. E. Eliçabe, H. A. Larrondo, R. J. J. Williams, Light Scattering in the Course of a Polymerization-Induced Phase Separation by a Nucleation and Growth Mechanism. *Macromolecules* **1998**, *31*, 8173–8182.

[17] L. Tsang, J. A Kong, K.-H. Ding, C. O. Ao, *Scattering of Electromagnetic Waves. Numerical Simulations*. John Willey & Sons, **2001**.

[18] W. K. Bertram, Correlation Effects in Small-Angle Neutron Scattering from Closely Packed Spheres. *J. Appl. Cryst.* **1996**, *29*, 682–685.

[19] C. Konák, J. Holuobek, P. Štepánek, A Time-Resolved Low-Angle Light Scattering Apparatus. Application to Phase Separation Problems in Polymer Systems. *Collect. Czech. Chem. Commun.* **2001**, *66*, 973–982.

